Photoactive Films of Photosystem I on Transparent Reduced Graphene Oxide Electrodes: Supporting Information

Preparation of RGO film

To prepare the reduced graphene oxide (RGO) electrode, we first functionalized the glass slide by soaking the glass in 1% aminopropyl triethoxysilane (APTES) in ethanol for 1 hour. We then washed the slide with ethanol. Previously, we tried washing the slide with water but this caused the slide to become opaque. Also, we originally cleaned the slide first with piranha solution, but eliminating this step did not appear to change the results and made the process much faster, safer, and easier. Then we spin coated graphene oxide (GO) onto the functionalized glass slide. We used 500 µL of 5 mg/mL GO in ethanol and spin coated at 800 rpm for 4 min. Originally, we tried to spin coat the GO out of water, but the resulting film was extremely uneven. We then reduced the GO film via a hydrazine vapor reduction method. We placed the GO coated slides in a small petri dish and then placed this small petri dish in a larger petri dish that also contained 1 mL of hydrazine. We covered the larger petri dish and heated it to 30 °C for 3 hrs. The color change from light brown to dark grey visibly indicates the reduction of the GO. The following figure summarizes the method and parameters for the RGO film preparation (SFigure 1).

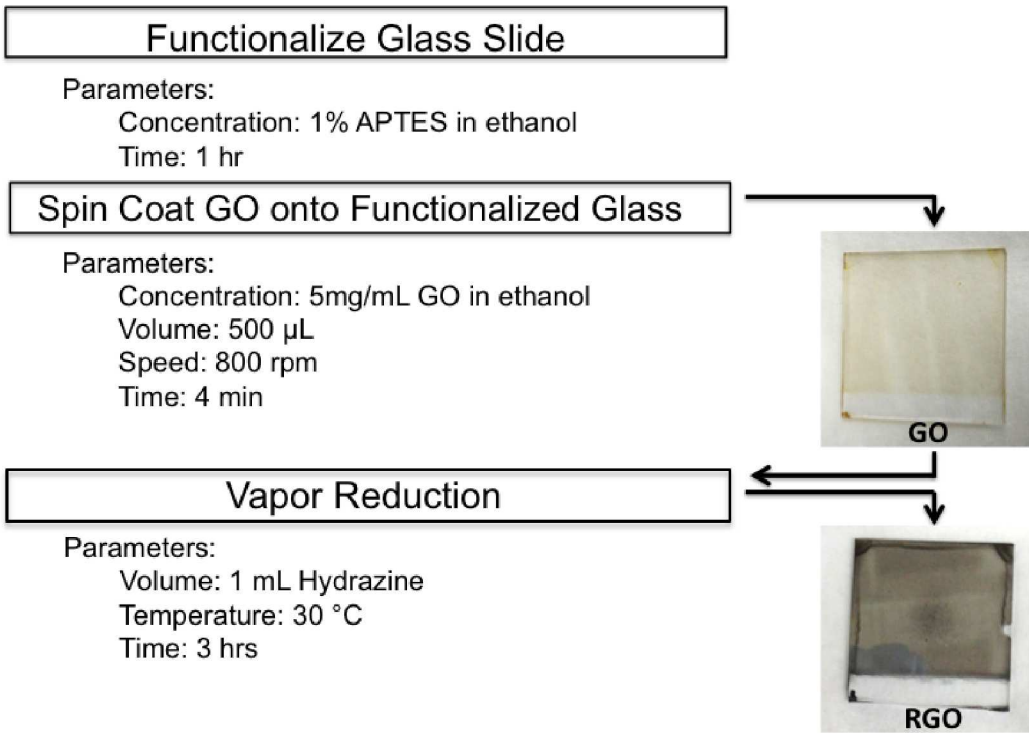

SFigure 1. Flow chart summarizing the method for preparing the RGO film and the specific parameters.

Characterization of RGO film

The resulting RGO film was characterized by its thickness, resistance, Raman peak shift, absorbance, and cyclic voltammetry (CV). We used profilometry to measure the thickness of the RGO films (SFigure 2). We scanned across a 2 mm section of the edge of the film for a duration of 100 seconds. While moderately uneven, the approximate thickness of the RGO film was 50 nm. We measured the resistance of the RGO film using a four point probe resistivity measurement. The average resistance from three measurements was 4.8 ± 1.7 kΩ. The resistance of the GO before reduction was too high to measure. These results support our previous reasoning that graphite loses conductivity when it is oxidized to GO but can regain this conductivity when it is reduced.

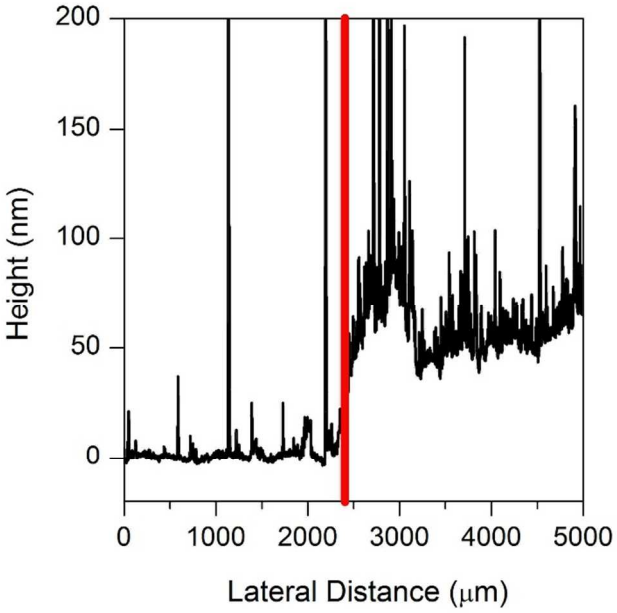

SFigure 2. Profilometry scan of the RGO electrode. The solid red line indicates the edge of the RGO film. Note both the film height (~50 nm) and the film roughness.

We measured the Raman spectra of GO and RGO (SFigure 3). The D/G peak intensity increases from 1.08 with GO to 1.61 with RGO. This ratio is calculated by dividing the peak at approximately 1350 cm^{-1} (D peak) by the peak at approximately 1600 cm^{-1} (G peak). The increase of the D/G ratio indicates the reduction of the GO film.

We used UV-Vis spectroscopy to measure the absorbance of the RGO film. The absorbance of the film increased four-fold when we reduced the GO.

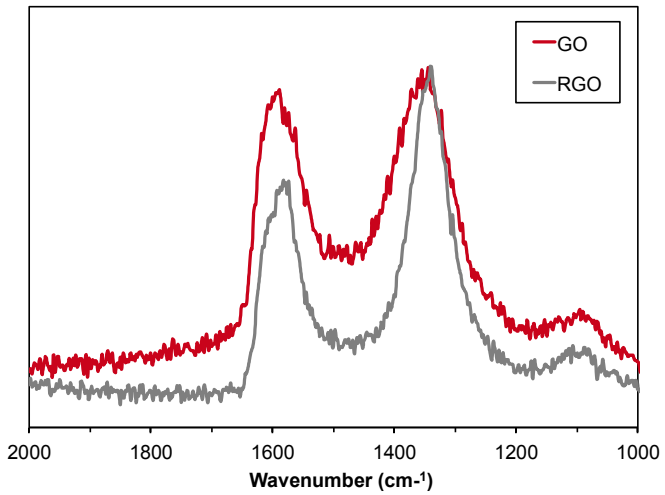

SFigure 3. Raman spectra of RGO and GO. The D peak occurs at approximately 1350 cm-1 and the G peak occurs at approximately 1600 cm^{-1}.

The CV scan of the RGO electrode shows both reduction and oxidation of the mediator solution, which indicates reversibility of electron flow in the electrode (SFigure 4). The RGO electrode required a fairly slow scan rate (1 mV/s) due to a slower flow of electrons through the RGO.

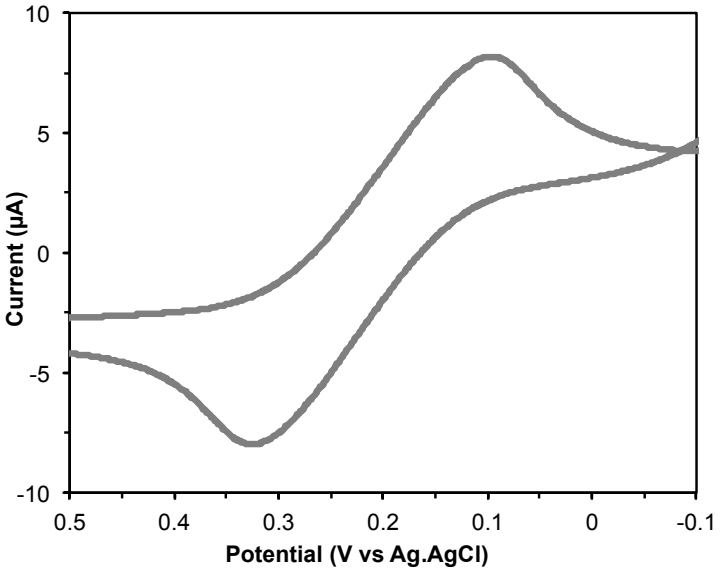

SFigure 4. Cyclic Voltametry of a RGO electrode in 1 mM ferricyanide/1 mM ferrocyanide mediator solution, with 100 mM KCL as the supporting electrolyte, Ag/AgCl as the reference electrode, and platinum mesh as the counter electrode. The scan rate was 1 mV/s.

PSI Deposition

To prepare the photosystem I (PSI) modified RGO electrode, we deposited 50 µL of dialyzed PSI on a 0.283 cm^2 circle of RGO and applied a vacuum to remove the solvent. We repeated this process two more times to achieve a thick, continuous film of PSI on the RGO. Using profilometry, we determined the resulting film of PSI to be roughly 350 nm thick. We can see both visibly and from the UV-Vis spectra that the PSI was indeed deposited of the RGO (SFigure 5). The PSI-modified RGO electrode shows the characteristics peaks of PSI. The PSI-modified RGO electrode has higher absorbance than PSI on glass alone due to the additional absorbance by the RGO.

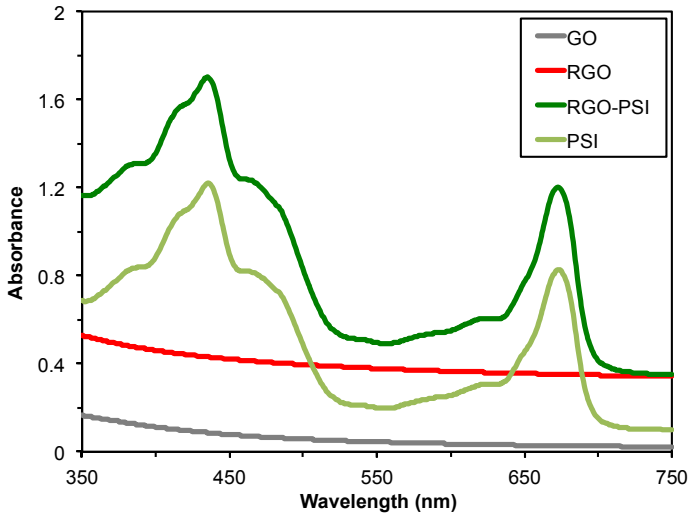

SFigure 5. UV-Vis spectra of PSI-modified RGO film (dark green), PSI film on unmodified glass (light green), unmodified RGO film (black), and GO film (red).

Experimental Set-up

We performed photochronoamperometric measurements on the photodiode to determine the photocurrent density. The half cell set-up consisted of the PSI-modified RGO as the active electrode, Ag/AgCl as the reference electrode, platinum mesh as the counter electrode, and various mediator solutions with 100 mM KCl as the supporting electrolyte (SFigure 6). Due to the

transparency of the RGO film, we are able to illuminate the active electrode directly through the RGO electrode instead of directing the light through the mediator solution. When light shines through the PSI-modified RGO electrode, electrons flow from the mediator solution to the PSI-modified RGO electrode and the mediator is oxidized.

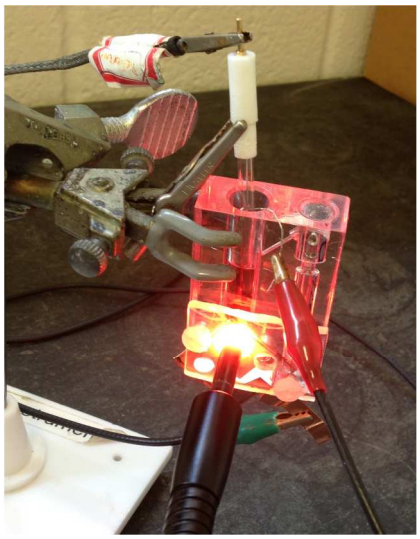

SFigure 6. Half-cell set-up with the PSI-modified RGO as the active electrode, platinum mesh as the counter electrode, and Ag/AgCl as the reference electrode. The photoelectrode is illuminated directly instead of directing the light through the mediator solution.

Open Circuit Potential Measurements

During the photochronoamperometric experiments we held the working electrode at the experimentally determined open circuit potential in order to ensure that the measurements were performed with an overpotential of 0 V. As seen in the STable 1, the open circuit potential shifts as different electrochemical mediators are used, as expected. Additionally, the addition of the PSI film has little effect on the open circuit potential in most cases. This differs from our previous measurements using semiconducting electrodes, where the addition of the PSI multilayer film impacts the open circuit potential more significantly. This difference is likely due to the effects of band-bending that occurs when semiconducting electrodes are used.

Mediator	Concentration	PSI Film	OCP Average	Stdev
Ferri/ferro-cyanide	2 mM	No	0.208	0.007
Ferri/ferro-cyanide	2 mM	Yes	0.207	0.007
Sodium Ascorbate	2 mM	No	-0.055	0.024
Sodium Ascorbate	2 mM	Yes	-0.025	0.037
Ruthenium hexamine (II)	2 mM	No	-0.073	0.073
Ruthenium hexamine (II)	2 mM	Yes	-0.059	0.062
Ruthenium hexamine (II)/(III)	2 mM	No	-0.016	0.015
Ruthenium hexamine (II)/(III)	2 mM	Yes	0.059	0.088
Methylene Blue	2 mM	No	0.059	0.056
Methylene Blue	2 mM	Yes	0.050	0.042
Methyl Viologen	2 mM	No	0.047	0.024
Methyl Viologen	2 mM	Yes	0.018	0.023
DCPIP	2 mM	No	0.017	0.019
DCPIP	2 mM	Yes	0.047	0.015
DCPIP	0.2 mM	No	0.104	0.032
DCPIP	0.2 mM	Yes	0.099	0.025
DCPIP	10 mM	No	0.057	0.005
DCPIP	10 mM	Yes	0.080	0.012
DCPIP	20 mM	No	0.055	0.005
DCPIP	20 mM	Yes	0.043	0.031

STable 1. List of the average open circuit potential (OCP) for various electrochemical systems used in the main text. System with a multilayer film of PSI are highlighted in green.

Photovoltage Measurement

While the focus of the manuscript was on the improved photocurrent density of a PSI modified RGO electrode, it is important to know the photovoltage for photovoltaic applications. The photovoltage measurement for a PSI modified RGO electrode is presented in SFigure 7. The photovoltage of the biohybrid electrode is roughly 14 mV. This low photovoltage contributes to the low quantum efficiency (2.9×10^{-4} %). We expect that this photovoltage can be significantly improved, however, by using a different counter electrode and orienting the PSI complexes within

the film. Further improvements in the photocurrent production will provide additional improvement to the quantum efficiency as we have observed over the past 10 years of research in this field.

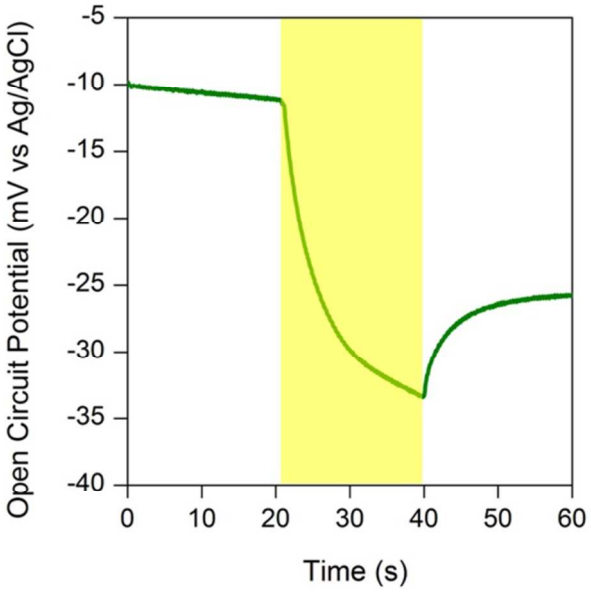

SFigure 7. Photovoltage measurement of a PSI modified RGO electrode using 2 mM DCPIP and 100 mM KCL as the electrochemical mediator. The photovoltage was determined by the change in the open circuit potential as the system changed from a dark to an illuminated condition (20-40 s).

Photoactivity of electrochemical mediators

During the course of our experiments, we were surprised by relatively high photocurrent densities produced during our control experiments. In order to determine if the photocurrent was produced by the RGO electrode or by the electrochemical mediator itself, we performed photochronoamperometric experiments using an fluorine doped tin oxide (FTO) electrode in place of the RGO electrode. As seen in SFigure 8, DCPIP demonstrates a significant amount of photocurrent in the absence of RGO or PSI. The photocurrent production does not account for all of the photocurrent observed in our RGO control electrode described in the main text, implying that the RGO also contributes to the photocurrent density of the system. This interesting finding suggests that the biohybrid electrode is able to synergistically interact with the DCPIP mediator to

generate higher photocurrent densities than would be possible for the components individually. We also found that the other mediators demonstrated photocurrent density upon illumination, although the RGO electrode appeared to be the more dominate contributor in these cases.

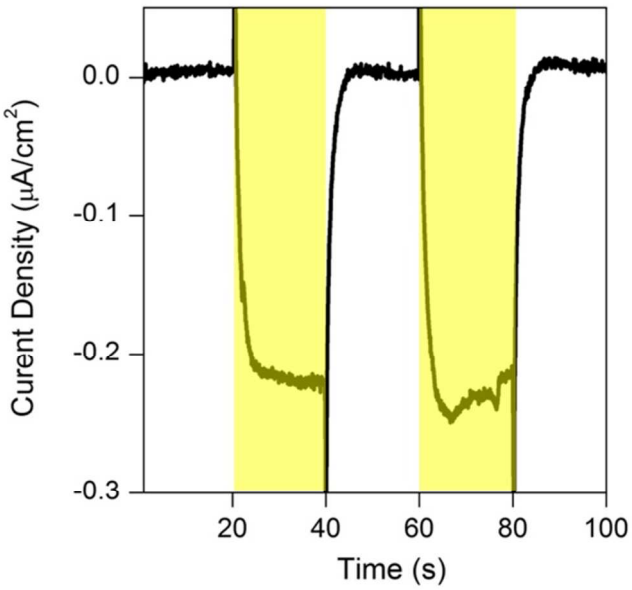

SFigure 8. Photochronoamperometry of DCPIP using an FTO electrode. The electrochemical mediator consisted of 2 mM DCPIP and 100 mM KCl. The sample was illuminated from 20-40 seconds and 60-80 seconds as indicated by the shaded areas.

Comparison of Photocurrent Generation

In STable 2 we compare the photocurrent generation from the current manuscript with other publications.

Photocurrent (uA/cm^2)	Electrode	PSI film type	Mediator	Reference
5	Reduced Graphene Oxide	Multilayer	20 mM dichloroindophenol	current
0.55	Graphene	Monolayer	20 mM methylene blue	1
0.1	Carbon Nanotubes on Gold	Monolayer	N/A	2
7.9	Gold	Multilayer	0.2 mM Ferri/Ferro-cyanide	3
0.075	Gold	Monolayer	0.25 mM Methyl Viologen, 0.0135 mM $Os(bpy)_2Cl_2$	4
29	Redox Polymer on Gold	Embedded	2 mM Methyl Viologen	5
362	nanostructured ZnO	Monolayer	500 mM $Co(Ophen)_3$(bis(trifluoromethanesulfonyl)imide)$_2$	6
875	p-doped Silicon	Multilayer	200 mM Methyl Viologen	7

STable 2. Comparison of photocurrent production using various electrodes, film types, and mediators as reported in the literature.

References

(1) Gunther, D.; LeBlanc, G.; Prasai, D.; Zhang, J. R.; Cliffel, D. E.; Bolotin, K. I.; Jennings, G. K. Photosystem I on Graphene as a Highly Transparent Photoactive Electrode. *Langmuir* **2013**, *29*, 4177–4180.

(2) Carmeli, I.; Mangold, M.; Frolov, L.; Zebli, B.; Carmeli, C.; Richter, S.; Holleitner, A. W. A Photosynthetic Reaction Center Covalently Bound to Carbon Nanotubes. *Adv. Mater.* **2007**, *19*, 3901–3905.

(3) Ciesielski, P. N.; Faulkner, C. J.; Irwin, M. T.; Gregory, J. M.; Tolk, N. H.; Cliffel, D. E.; Jennings, G. K. Enhanced Photocurrent Production by Photosystem I Multilayer Assemblies. *Adv. Funct. Mater.* **2010**, *20*, 4048–4054.

(4) Manocchi, A. K.; Baker, D. R.; Pendley, S. S.; Nguyen, K.; Hurley, M. M.; Bruce, B. D.; Sumner, J. J.; Lundgren, C. A. Photocurrent Generation from Surface Assembled Photosystem I on Alkanethiol Modified Electrodes. *Langmuir* **2013**, *29*, 2412–2419.

(5) Badura, A.; Guschin, D.; Kothe, T.; Kopczak, M. J.; Schuhmann, W.; Rögner, M. Photocurrent Generation by Photosystem 1 Integrated in Crosslinked Redox Hydrogels. *Energy Environ. Sci.* **2011**, *4*, 2435–2440.

(6) Mershin, A.; Matsumoto, K.; Kaiser, L.; Yu, D.; Vaughn, M.; Nazeeruddin, M. K.; Bruce, B. D.; Graetzel, M.; Zhang, S. Self-Assembled Photosystem-I Biophotovoltaics on Nanostructured TiO2 and ZnO. *Sci. Rep.* **2012**, *2*.

(7) LeBlanc, G.; Chen, G.; Gizzie, E. A.; Jennings, G. K.; Cliffel, D. E. Enhanced Photocurrents of Photosystem I Films on P-Doped Silicon. *Adv. Mater.* **2012**, *24*, 5959–5962.